



1 **A Sedimentary Carbon Inventory for a Scottish Sea Loch**
2 **(Fjord): An Integrated Geochemical and Geophysical**
3 **Approach.**

4
5 **C. Smeaton¹, W. E. N. Austin^{1,2}, A. L. Davies¹, A. Baltzer³, R. E. Abell² and J. A.**
6 **Howe².**

7 [1]{School of Geography & Geosciences, University of St-Andrews, St-Andrews, KY16
8 9AL, UK}

9 [2]{Scottish Association for Marine Science, Scottish Marine Institute, Oban PA37 1QA,
10 UK}

11 [3]{Institut de Géographie et d'Aménagement Régional de l'Université de Nantes, BP 81 227
12 44312 Nantes cedex 3}

13 Correspondence to: C. Smeaton (cs244@st-andrews.ac.uk)

14

15 **Abstract**

16 Quantifying sedimentary carbon stocks in the coastal ocean is key to improving our
17 understanding of long-term storage of carbon in the coastal ocean and to further constraining
18 the global carbon cycle. Here we present a methodological approach which combines seismic
19 geophysics and geochemical measurements to quantitatively estimate the total stock of carbon
20 held within marine sediment. Through the application of this methodology to Loch Sunart a
21 sea loch (fjord) on the west coast of Scotland we have created the first sedimentary carbon
22 inventory for a fjordic system. The sediment of Loch Sunart holds 26.88 ± 0.52 Mt of carbon
23 split between 11.05 ± 0.23 Mt and 15.02 ± 0.35 Mt of organic and inorganic carbon
24 respectively. This quantitative estimate of carbon stored in Loch Sunart is significantly higher
25 than previous estimates. Through comparison to Scottish peatland carbon stocks we have
26 determined that Loch Sunart on a per are basis is a significantly more effective store of
27 carbon. This initial work supports the concept that fjords are important environments for the
28 burial and long-term storage of carbon and therefore should be considered as unique
29 environments while considering coastal carbon stocks.



1 **1 Introduction**

2 The rising prominence of Blue Carbon, i.e. carbon (C) which is stored in coastal ecosystems,
3 notably, mangroves, tidal marshes, seagrass meadows and sediments has forced a
4 reassessment of our knowledge of C in the coastal ocean (Nellemann et al., 2009). In recent
5 years there have been a number of reviews (Bauer et al., 2013 & Cai et al., 2011) highlighting
6 knowledge gaps and the limited understanding of both the C sources and sinks in the coastal
7 ocean (Bauer et al. 2013). Quantifying the stores of C in the coastal ocean is the first step to a
8 better understanding of coastal carbon dynamics. Global C burial in the coastal zone is
9 estimated in the region of 237.6 Tg yr⁻¹ with approximately 126.2 Tg yr⁻¹ of C being buried in
10 depositional areas i.e. estuaries and the shelf (Duarte et al., 2005). The lack of regional and
11 national coastal sedimentary C inventories means these global estimates cannot be confirmed
12 or further constrained.

13

14 One of the rare examples of a national marine C inventory was carried out by Burrows et al.
15 (2014) producing initial estimates of Blue Carbon in Scottish territorial waters; they
16 calculated that these waters stored 1,757 Mt C, with coastal and offshore sediments acting as
17 the main repositories. Burrows et al. (2014) suggested that the majority of this organic carbon
18 (OC) was held in sea loch (fjord) sediments.

19 It has been long known that fjords are important stores of C (Syvitski et al., 1987) and that C
20 burial in sediments is the most significant mechanism of long-term (>1000years) OC
21 sequestration in the coastal ocean setting (Hedges et al., 1995).. The work by Smith et al.
22 (2015) has also shown that globally fjordic systems act as a CO₂ “buffer” by efficiently
23 capturing and burying labile terrestrially derived OC and preventing it from entering the
24 adjacent ocean system where it is prone to recycling. These authors have calculated that 11%
25 of annual global marine carbon sequestration occurs within fjords.

26 Despite these findings, much of the global research to assess and quantify C stocks is
27 disproportionately skewed towards the terrestrial environment (e.g. Yu et al., 2010). This
28 trend is also found at the regional scale where there have been multiple studies quantifying
29 the carbon held within Scottish soils (Aitkenhead et al., 2016, Bradley et al., 2005, &
30 Chapman et al., 2013) and peats (Aitkenhead et al., 2016, Howard et al., 1995, Cannell et al.,
31 1999 & Chapman et al. 2009).



1 In addition to the challenges of access and cost to sample these environments when compared
2 to the adjacent terrestrial environment, it might also be argued that the sparsity of marine
3 sedimentary C inventories is due to the lack of a robust methodology to quantify these C
4 stores. Syvitski et al. (1987) commented that “the development of a methodological approach
5 to quantify the C in the sediment of a fjord must be a priority”, yet in the subsequent years
6 there has been relatively little progress towards this goal.

7 The absence of a robust methodology to quantify the C held in marine sediments is illustrated
8 by Burrows et al. (2014), who estimated that there is 0.34 Mt OC stored in the sediments of
9 Scottish sea lochs (fjords). However, these calculations only take into account an estimate of
10 OC in the top 10 cm of sediment, despite the fact that sediment depths of >25 m are common
11 in Scottish sea lochs (Baltzer et al., 2010, Howe et al. 2002). Therefore, it is likely that current
12 best estimates of the quantity of OC has been significantly underestimated and that the
13 presence of significant quantities of inorganic carbon (IC) held within sea lochs sediments has
14 been overlooked.

15 This study combines geochemical, geophysical and geochronological techniques to produce a
16 methodology capable of delivering quantitative first-order calculations of the mass of C stored
17 within the sediment of a sea loch and, potentially, of achieving the goal set out by Syvitski et
18 al. (1987). This work provides the first carbon inventory for a fjord and further develops the
19 concept of these fjords as being globally important sites for the burial of C as set out by Smith
20 et al. (2015).

21 **2 Material & Methods**

22 **2.1 Study Area**

23 Loch Sunart is a sea loch on the West coast of Scotland (Fig.1). The loch is 30.7 km long and
24 covers an area of 47.3 km² with a maximum depth of 145 m. It consists of three basins
25 separated by shallower, rock sills. The inner basin is separated from the middle basin by a sill
26 at approximately 6 m depth, while the middle and outer basins are separated by a sill at
27 approximately 31 m depth (Edwards & Sharples, 1986; Gillibrand et al., 2005). The silled
28 nature of the bathymetry allows the loch to act as a natural sediment trap for both terrestrial
29 and marine derived materials (e.g. Nørgaard-Pedersen et al., 2006).

30 Loch Sunart's catchment covers 299 km²; the main tributaries of the loch are the Rivers
31 Carnoch and Strontain; the latter has a mean daily discharge of 1409 m³ (2009-2013). The



1 mean annual precipitation in Loch Sunart's catchment is 2632 ± 262 mm (Capell et al., 2013).
2 The combination of small catchment size and high precipitation means that the flow network
3 is sensitive to precipitation changes which can result in a flashy flow regime (Gillibrand et al.,
4 2005).

5 The catchment is largely dominated by high relief and poorly developed soils. The bedrock
6 consists primarily of igneous and metamorphic rocks, overlain by gley and podzol soils with
7 limited peat in the upper catchment (Soil Survey of Scotland., 1981). Exposed rock is
8 common on the steep slopes; much of the catchment's vegetation can be found by streams or
9 on the loch shore and is dominated by both commercial forestry and natural woodlands; there
10 is only very limited agriculture within the catchment. The combination of steep, exposed
11 slopes, poorly developed soil, a reactive river network and poorly developed vegetation
12 typically results in high surface runoff and sediment transport (Hilton et al., 2011).

13 The characteristics of Loch Sunart and its catchment are representative of sea lochs across
14 mainland Scotland (Edwards & Sharples., 1986), with the possible exception of Loch Etive
15 which has a hypoxic upper basin (Friedrich et al., 2014). The sea lochs of the Scottish Islands
16 (Shetland, Orkney & the Western Isles) differ from their mainland counterparts in that they
17 are generally shallower and have catchments characterised by lower relief and are largely
18 dominated by peat or peaty soil (Soil Survey of Scotland., 1981). Syvitski and Shaw's (1995)
19 table of generalised fjord characteristics allows us to compare the sea lochs of mainland
20 Scotland to other fjordic systems globally. The fjords of the Norwegian mainland, Canada and
21 the Fiordland, New Zealand (Hinojosa et al., 2014) are characterised by similar climate,
22 geomorphology, river discharge, basin water temperature and sedimentation rate as the sea
23 lochs of Scotland. The fjords of mainland Scotland differ significantly from those in
24 Greenland, Alaska, Svalbard and the Canadian Arctic, many of which still have active
25 glaciers, resulting in very different sediment input regime.

26 **2.2 Seismic Data Acquisition and Processing**

27 **2.2.1 Data Acquisition**

28 A seismic geophysical survey of Loch Sunart took place in 2002 aboard the RV *Envoy*
29 (Fig.2). A Seistec Boomer System was used to create seismic profile data throughout the loch.
30 The data were recorded using an Elics-Delph data acquisition system coupled to the
31 Differential Global Positioning System (DGPS). The Boomer system operated on a frequency



1 of 1 to 10 kHz and had a pulse duration of 75 to 250 ms at a power of 150 J. The system has a
2 depth resolution of 25 cm and can penetrate 100 m in soft sediment (Simpkin & Davies
3 1983). A total of 34 transects of the loch were acquired (Fig.2). The survey achieved an
4 average penetration of 50 m; gas blanking prevented the signal from penetrating the sediment
5 in some areas (Baltzer et al., 2010).

6 2.2.2 Defining Sedimentary Horizons

7 Each seismic profile was combined with the DGPS data and processed with the Petrel
8 (Schlumberger) software package. Subsequent analysis was undertaken using the open source
9 SeiSee (DMNG) software package. Initial interpolation, following Baltzer et al.'s (2010)
10 methodology, defined the different seismic horizons (H) and the layers between the horizons
11 which are defined as seismic units (U) numbered 1 to 3 from the basement horizon upwards
12 (Fig 3). The compilation of the horizons and units allows the construction of an equivalent
13 seismic stratigraphy for each sediment core and the loch as a whole.

14 Using SeiSee, points were picked along each of the four horizons creating polylines. Each
15 polyline was split into points at 0.25 m intervals and each point was assigned an x,y,z
16 coordinate that represents its geographic location and depth (relative to mean sea level).

17 2.3 Sediment Sampling

18 Eight sediment cores (Table.1) were collected from Loch Sunart (Fig.1) in 2001 using a
19 gravity corer (GC) as part of the HOLSMEER project. This was supplemented with further
20 sampling on a follow-up cruise on-board the *RV Calanus* in August 2013 where a short GC
21 was collected to fill a gap between the original coring sites. These cores capture the post-
22 glacial history of sediment accumulation within the loch, as confirmed by ^{14}C basal dates.
23 Additionally, we accessed the lower sections of core MD04 2833 which was recovered using
24 the CALYPSO giant piston corer from the *RV Marion Dufresne* in July 2004 as part of the
25 IMAGES project. Sampling of Section VIII (1050-1200 cm) of MD04 2833 was undertaken
26 to obtain sediment of inferred glacial origin for geochemical analysis (Baltzer et al., 2010).



1 **2.4 Sediment Analysis**

2 **2.4.1 Physical Characteristics**

3 Detailed sediment logging was undertaken for each of the cores (Supplementary Material).
4 The gravity cores were sub-sampled at 10 cm intervals and high resolution sampling at 1 cm
5 intervals was undertaken on the short core. Section VIII of glacial sediment core MD04-2833
6 was sub-sampled at 12 cm intervals. Each sub-sample was split for physical property and
7 geochemical analyses. The wet (WBD) and dry bulk density (DBD) of the sediment was
8 calculated following Dadey et al. (1992).

9 **2.4.2 Bulk Elemental Analysis**

10 To quantify the total carbon (TC) content, each sub-sample was freeze-dried and milled to a
11 fine powder. A 20 ± 2 mg aliquot was placed in a tin capsule and measured on a COSTECH
12 Elemental Analyser (EA) calibrated with acetanilide (Verardo et al, 1990, Nieuwenhuize et al.,
13 1994). Precision of the analysis is estimated from repeat analysis of standard reference
14 material B2178 (Medium Organic content standard, Elemental Micro analysis, UK) C =
15 0.07% N = 0.02% (n = 8).

16 To quantify OC, the process was repeated with the addition of H_2SO_3 to remove the inorganic
17 carbon (IC). After acidification vessels were placed in a vacuum desiccator to remove any
18 remaining CO_2 and the sample was then freeze-dried to remove the H_2SO_3 . IC was calculated
19 from the difference between TC and OC measurements. The mean standard deviation of TC
20 and OC triplicate measurements (n=10) were 0.04 %, 0.17 % respectively.

21 **2.4.3 Sediment Geochronology**

22 Basal radiocarbon dates for five of the gravity cores were obtained by accelerator mass
23 spectrometer (AMS) radiocarbon dating of marine carbonate material (mollusc). This was
24 carried out at the University of Aarhus, Denmark (AAR), Centre of Accelerator Mass
25 Spectrometry, USA (CAMS) and the NERC Radiocarbon Laboratory, Scotland (SUERC).
26 The radiocarbon dating was used to validate the Holocene chronology of the seismic
27 stratigraphy. A single MD04-2833 sample was processed at Laval University, Canada (UL) to
28 confirm that the sediment was early post-glacial in age. Dates were calibrated using OxCal
29 4.2.4 age modelling software (Bronk Ramsey., 2009 & Bronk Ramsey & Lee., 2013)



1 applying the Marine13 curve (Reimer et al., 2013) and the regional marine radiocarbon
2 reservoir age correction: ΔR value of -26 ± 14 yr (Cage et al. 2006).

3 Sediment accumulation rates (SAR) were calculated as an approximation for the whole core
4 using basal ages and a linear interpolation to the core top, assuming a contemporary surface.
5 We recognise that the calculations will be crude and do not take into consideration factors
6 such as compaction and possible changes in sedimentation rate, but these calculations provide
7 initial insight into the variability of SARs within the loch and allow first-order C
8 accumulation rates to be estimated.

9 **2.5 Sediment Quantification & Characterisation**

10 **2.5.1 Digital Terrain Models (DTM)**

11 The points collected from each seismic horizon were connected to form a DTM of that
12 horizon. This was achieved using spatial modelling techniques in ArcGIS. The compiled x,y,z
13 data were statistically tested to determine the gridding technique best suited to the
14 interpolation of the data. Eleven gridding techniques were subjected to cross validation
15 (Chiles & Delfiner 1999)(Supplementary Material).. The residual Z mean value and standard
16 deviation were examined; the technique with the lowest residual Z mean and standard
17 deviation for each horizon (and the data set as a whole) was chosen as the gridding technique
18 best suited to the interpolation of the data. Kriging (with linear interpolation) (Cressie, 1990)
19 with a 100 by 1000 node structure performed best and was chosen to create computationally
20 efficient DTMs for each seismic horizon.

21 **2.5.2 Volumetric Calculations**

22 The horizon DTM grids were used to calculate the volume of sediment in each seismic unit
23 and, by extension, within the loch as a whole. By subtracting one DTM grid from another
24 (e.g. Surface DTM – Bedrock DTM) the volume between the grids was calculated. Three
25 different numerical integration algorithms were used for this calculation (Eq.1,2,3). The net
26 volume is reported as the mean of these three calculations. In the following formulae Δx
27 represents the grid column spacing, Δy represents the grid row spacing and G_{ij} represents the
28 grid node value in row i and column j (Press et al., 1988).

29 *Trapezoidal Rule*



1 The pattern of coefficients is $\{1,2,2,2,\dots,2,2,1\}$: (1)

$$2 \quad A_i = \frac{\Delta x}{2} [G_{i,1} + 2G_{i,2} + 2G_{i,3} \cdots + 2G_{i,nCol-1} + G_{i,nCol}]$$

$$3 \quad \text{Volume} \approx \frac{\Delta y}{2} [A_1 + 2A_2 + 2A_3 + \cdots + 2A_{nCol-1} + A_{nCol}]$$

4 *Extended Simpson's Rule*

5 The pattern of coefficients is $\{1,4,2,4,2,4,2,\dots,4,2,1\}$: (2)

$$6 \quad A_i = \frac{\Delta x}{3} [G_{i,1} + 4G_{i,2} + 2G_{i,3} + 4G_{i,4} + \cdots + 2G_{i,nCol-1} + G_{i,nCol}]$$

$$7 \quad \text{Volume} \approx \frac{\Delta y}{3} [A_1 + 4A_2 + 2A_3 + 4A_3 + \cdots + 2A_{nCol-1} + A_{nCol}]$$

8 *Extended Simpson's 3/8 Rule*

9 The pattern of coefficients is $\{1,3,3,2,3,3,2,\dots,3,3,2,1\}$: (3)

$$10 \quad A_i = \frac{3\Delta x}{8} [G_{i,1} + 3G_{i,2} + 3G_{i,3} + 2G_{i,4} + \cdots + 2G_{i,nCol-1} + G_{i,nCol}]$$

$$11 \quad \text{Volume} \approx \frac{3\Delta y}{8} [A_1 + 3A_2 + 3A_3 + 2A_3 + \cdots + 2A_{nCol-1} + A_{nCol}]$$

12

13 2.5.3 Sediment Mass Quantification

14 The mean dry bulk density (DBD) for each seismic unit was calculated and assigned to the
 15 equivalent seismic units within each core. The spatial distribution of the DBD for each
 16 seismic unit was modelled, again using Kriging (with linear interpolation). The resulting
 17 contour plot was integrated with the volumetric model for each seismic unit to calculate the
 18 dry mass of the sediment held within that seismic unit. The integration process calculates the
 19 volume of sediment held within each of the DBD contours and multiplies that volume with
 20 the associated DBD value to calculate the mass of sediment.

21 2.5.4 Sedimentary Carbon Quantification

22 The same methodology used to integrate the volume and density data was used to combine
 23 bulk elemental data with the sediment dry mass calculations. Mean values for TC, OC and IC
 24 in each seismic unit were assigned to the seismic units from the available core data. Kriging
 25 (with linear interpolation) was again used to create contour maps representing the quantity of
 26 TC, OC and IC in each seismic unit and the mass of sediment held between the contours was
 27 multiplied by the percentage of the element quantifying the mass of TC, OC and IC held



1 within the loch's sediment. Finally, we calculated how effectively the loch stores C (C_{eff}) as a
2 depth-integrated average value per km^2 for both the post-glacial and glacial derived
3 sediments. This measure allows the loch's C stores to be directly compared with other C
4 stores (peatlands, soil, etc.).

5 **3 Results**

6 **3.1 Seismic Interpretation**

7 **3.1.1 Seismic Horizons and Units**

8 Four horizons were identified throughout the loch (Fig.3): these represent the basement (H1)
9 and the sediment water interface (H4) with two intermediate horizons (H2 & H3). Core
10 stratigraphy (Baltzer et al. 2010) indicates that H2 divides the post-glacial and glacial
11 sediment; while H3 splits the post-glacial sediment into two units. The seismic data displays a
12 fifth horizon between H1 and H2 which is only present in the inner basin and partially in the
13 middle basin. We interpret this as glacial sediment from the Younger Dryas, as confirmed by
14 radiocarbon dating (Baltzer et al., 2010, Mokeddem et al. 2010); for the purposes of this
15 paper, the horizon was amalgamated with H2.

16 A seismic stratigraphy was developed based on these horizons (Fig.3). U1 is interpreted as
17 glacial sediment based on the observation of the short, discontinuous seismic reflections
18 which are synonymous with poorly sorted material; the unit varies in thickness but never
19 drops below a minimum thickness of 10 m. U2 is found throughout the loch with an average
20 thickness of 5 – 10 m; the unit drapes over U1. U3 is the uppermost unit and has a
21 homogenous thickness of around 1m; it is characterised by laminated acoustic reflections.
22 Both U2 and U3 are interpreted as post-glacial infill of the loch; though clear in the seismic
23 geophysics the boundary between U2 and U3 is poorly defined in the sediment lithology
24 (Supplementary Material). Similar patterns in seismic stratigraphy have been observed
25 throughout the west coast of Scotland (Binns et al., 1974a, b, Boulton et al., 1981 and Howe
26 et al., 2002).

27 We compared our interpretation of the seismic data to the seismic interpretation of Baltzer et
28 al., (2010); this exercise was designed to test the replicability of our interpretation and allow
29 potential uncertainties in the seismic interpolation to be built into our future applications. The



1 comparison identified small differences in the depth of H1 (-0.17 m), H2 (+0.34) & H3 (-0.22
2 m). These differences were integrated into the volumetric calculations as an error term.

3 3.2 Sediment Geochronology

4 Calibrated radiocarbon dates for the gravity cores (Table.2) indicate that these cores are
5 comprised of sediment accumulated during the post-glacial period (Holocene). The age of the
6 deeper basal sediment of MD04-2833(Section VIII) was confirmed through dating of a
7 mollusc (*Pecten maximus*); the calibrated age was 17041 ± 312 cal BP which, combined with
8 the characteristic glacial core lithology of poorly sorted sedimentary material, indicates that
9 this basal sediment of MD04-2833 was deposited by the retreat of the British ice sheet (BIS)
10 at the end of the last glacial period 13500 to 17000 cal BP (Clark et al., 2010, Scourse et al.,
11 2009, Wilson et al. 2002).

12 Through comparison of the chronologies to the seismic stratigraphy we can test the
13 interpolation and further constrain the age of each seismic unit. The seismic unit for the
14 equivalent depth of each of the radiocarbon samples has been compiled (Table.2), then
15 compared to the seismic unit that the sample would fall into based on age alone as per the
16 Baltzer et al. (2010) chronostratigraphy. Of the 18 samples tested, 15 have a matched pair of
17 seismic units; the three that do not have corresponding seismic units are all from GC023,
18 suggesting a problem with the dating of this core rather than the interpolation of the seismic
19 geophysics. This test signifies that our interpolation of the seismic geophysics is accurate and
20 that the chronostratigraphy developed for MD04-2833 (Baltzer et al., 2010) can be applied
21 throughout Loch Sunart. The seismic interpolation and the dated samples confirm that both
22 U2 and U3 are postglacial in origin. We can further constrain the age of the seismic units with
23 U2 representing the early to mid-Holocene and U3 mid to late Holocene in age.

24 SARs vary between the sedimentary basins, with the most rapid rates in the middle basin as
25 indicated by GC023 (0.12 ± 0.026 cm yr⁻¹). The inner basin has a similar SAR (0.089 ± 0.026
26 cm yr⁻¹) to the middle basin, but accumulation rates were significantly slower in the outer
27 basin, as illustrated by GC011 (0.017 ± 0.006 cm yr⁻¹).



1 3.3 Sediment Analysis

2 3.3.1 Bulk Density Measurement

3 Mean DBD was calculated for U1, U2 and U3 from each core. Figure 4 displays the DBD
4 results, which are arranged to mirror the spatial distribution of the cores, from the inner basin
5 to the outer basin. U1 sediment is characterised by the single section of MD04-2833, which
6 has a mean DBD of $2.19 \pm 0.09 \text{ g cm}^{-3}$. This is within the range of other northern hemisphere
7 fjords (Pedersen et al. 2012, Forwick et al. 2010 and Baeten et al. 2010). DBD increases down
8 each core as a result of sediment dewatering in response to compaction. GC011 is the only
9 core where U3 has a higher DBD than U2 most likely due to large quantities of shell in the
10 upper part of the core. U1 has the highest DBD; this reflects both the type of sediment
11 deposited during glacial retreat and long-term compaction over the post-glacial period.

12 3.3.2 Bulk Elemental Analysis

13 The mean quantity OC and IC has been calculated for U1, U2 and U3 (Fig.5). Again values
14 for U1 have been calculated using basal sediments of MD04-2833 (Section VIII). Clear
15 trends emerge from the data, with U3 always containing a greater quantity of OC than U2,
16 while the proportion of sedimentary OC generally decreases away from the inner basin. The
17 opposite is true for sedimentary IC, which generally increases away from the inner basin.
18 Sediment Quantification & Characterisation

19 3.3.3 Digital Terrain Models (DTMs)

20 The interpolation of the seismic profiles led to the creation of four DTMs (Fig.6) which
21 represent horizons H1 to H4. Both H4 and H3 follow the trajectory with minimal deviation,
22 primarily because U3 has a uniform depth of 1 m throughout the loch. Differences in depth
23 between H3, H2 and H1 are far more variable. The inner basin shows the least change in
24 depth between the horizons, although both H2 and H1 deepen before the sill (Fig.5). The
25 middle basin displays the greatest depth differences between the horizons and also where the
26 majority of the sediment is stored. Patterns in the outer basin are similar to those in the middle
27 basin, especially where the two meet. Horizon depths become less variable towards the
28 seaward direction.

29 To determine the accuracy of the models, the DTM for H4 was compared to an existing high-
30 resolution bathymetric model of the loch (Bates et al. 2004). The coordinates (x,y,z) of key



1 high and low points ($n=12$) were compared between surveys; the mean divergence between
2 surveys were calculated as x : -0.56 m , y : -0.81 , z : 0.21. Although the H4 DTM slightly
3 negatively offsets the x,y and overestimates the z coordinates of these points, the general
4 location and pattern of these seabed features compare favourably.

5 3.3.4 Volumetric Modelling

6 The DTMs and numerical integration algorithms were combined to calculate the volume of
7 sediment held within each seismic unit. This was further broken down by basin and into post-
8 glacial (U2 & U3) and glacial (U1) derived sediment (Table.3). The loch as a whole contains
9 a greater volume of glacial ($599731882 \text{ m}^3 \pm 1.89 \%$) than post-glacial sediment (530872293
10 $\text{m}^3 \pm 7.39 \%$). The outer basin is the only area where this trend is reversed. Comparison of the
11 three basins indicates that the middle basin contains the greatest combined (post-glacial +
12 glacial) volume of sediment ($30409301.04 \text{ m}^3 \pm 5.30 \%$) followed by the outer (16039257.2
13 $\text{m}^3 \pm 5.74 \%$) and inner basins ($4171662.46 \text{ m}^3 \pm 4.48 \%$).

14 3.3.5 Sediment Mass Quantification

15 The mean DBD for U2 and U3 were modelled (Fig.7) to determine the variability in spatial
16 distribution throughout the loch. A similar spatial pattern of DBD is found in both U2 and U3;
17 the DBD is lowest in the inner basin (U2: 0.47 g cm^{-3} , U3: 0.59 g cm^{-3}) rising out through the
18 middle basin where it peaks at 1.75 g cm^{-3} and 1.67 g cm^{-3} for U2 and U3 respectively. The
19 transition between the middle and outer basins is characterised with low DBD values (U2:
20 0.72 g cm^{-3} , U3: 0.91 g cm^{-3}); from this low point the DBD rises towards the seaward end of
21 the loch.

22 The model output was integrated with the volumetric data to calculate the mass of sediment
23 held within post-glacial sediment (Table 4). Since we have a single mean value for DBD for
24 U1 we applied this throughout the loch to calculate the mass of sediment held within this unit.
25 The loch holds a total of $1928.26 \pm 7.29 \text{ Mt}$ of sediment which is split into $652.09 \pm 6.62 \text{ Mt}$
26 of post-glacial and $1276.17 \pm 8.93 \text{ Mt}$ of glacial sediment. The inner basin holds the least
27 sediment followed by the outer basin with the middle basin acting as the main store of
28 sediment in Loch Sunart.



1 3.3.6 Sedimentary Carbon Quantification

2 Using a similar approach, the mean OC and IC were spatially modelled throughout the loch.
3 The output for U3 is illustrated in Figure 8. As before, the model outputs for U2 and U3 were
4 integrated with the sediment mass data in order to quantify the mass of TC, OC and IC held
5 within the post-glacial and glacial sediment (Table.4). Single mean values for TC, OC and IC
6 were again used to calculate their respective mass of C within the sediment of U1.

7 The sediment of Loch Sunart holds a significant quantity of C (26.88 ± 0.52 Mt) split between
8 OC (11.05 ± 0.23 Mt) and IC (15.02 ± 0.35 Mt). Though a greater mass of sediment is held
9 within the glacial sediment component, it is the post-glacial sediments which hold the largest
10 quantity of C (19.88 ± 0.27 Mt). The quantity of C held within each of Loch Sunart's basins
11 varies; the lowest amount is found in the inner basin (2.12 ± 0.45 Mt) followed by the outer
12 basin (6.70 ± 0.64 Mt). The sediment of middle basin holds significantly more C than both the
13 inner and outer basins combined; with 18.05 ± 0.66 Mt C stored in these sediments indicating
14 that the middle basin is the main repository for sedimentary C in Loch Sunart.

15 How effectively the loch stores C is measured by the C_{eff} (Table.5) and the OC:IC ratio. Loch
16 Sunart is characterised by an OC:IC ratio of 0.74 and has a C_{eff} of $0.568 \text{ Mt C km}^{-2}$, which can
17 be further broken down to a post-glacial C_{eff} of $0.42 \text{ Mt C km}^{-2}$ and a glacial C_{eff} of 0.148 Mt
18 C km^{-2} . The effective C storage can also be illustrated at the individual basin level with the
19 post-glacial sediments of the inner, middle and outer basins characterised by OC:IC ratios of
20 0.42, 1.00 and -0.42, illustrating the transition from OC as the dominant component of the
21 sediment in the upper loch to an IC-dominated sediment at the seaward end of the loch. The
22 middle basin is the most effective at storing post-glacial OC followed by the inner and outer
23 basin; similarly the middle basin is most effective at storing IC, but in contrast to the effective
24 storage of OC, the outer basin ranks second followed by the inner basin for IC. The glacial
25 material held within the loch as a whole is characterised by an OC:IC ratio of 0.42 with a
26 mean OC_{eff} 0.044 Mt km^{-2} and IC_{eff} 0.104 Mt km^{-2} .

27 3.4 A Methodology for Estimating Sedimentary Carbon and Attributing 28 Uncertainty Estimates

29 The joint geophysical and geochemical methodology outlined (Fig.9) provides a robust
30 approach to allow the first quantification of sedimentary C stocks in a fjord setting. An
31 important part of estimating sedimentary C stocks should be the quantification of uncertainty



1 associated with these estimates. There are several types of uncertainty that can influence
2 sedimentary carbon estimations (Fig.9), including interpolation, algorithmic, analytical,
3 sampling and extrapolation uncertainty. Several of these types of uncertainties are easily dealt
4 with statistically, for example the analytical uncertainties can be quantified through triplicate
5 measurements. The sampling uncertainty of a stratigraphic sequence (i.e. spatial variability of
6 C content in relation to sampling density) can be overcome by calculating the mean and
7 standard deviation to create composite values that are representative of the entire sediment or
8 seismic unit. We integrated the quantifiable uncertainties at each calculation step (Fig.4). By
9 calculating composite standard deviations we are able to propagate the uncertainties
10 throughout the C quantification process. In the interpolation of the seismic geophysics, it is
11 difficult to fully quantify the uncertainty involved in the process. Bond et al. (2007) set out a
12 5 step framework designed to reduce uncertainty in this process. We utilised the framework of
13 Bond et al. (2007) and additionally integrated a validation step using radiocarbon dating of
14 sedimentary cores (See Section 3.2). This allows us to reduce the uncertainties associated
15 with the seismic interpretation, although we recognise that some uncertainty remains (e.g.
16 highly variable patterns of depth) which cannot be fully quantified. Within this framework of
17 uncertainty, we consider our method to give a robust estimate for the carbon stocks present.

18 **4 Discussion: A new Sedimentary C Inventory for Scottish Coastal Waters**

19 The development of this methodology has allowed the estimation of the sedimentary C stocks
20 stored in Loch Sunart. The sediment which has been uncounted for within Loch Sunart holds
21 26.88 Mt C.

22 The only directly comparable estimation for sedimentary C stocks is the report by Burrows et
23 al. (2014), where they calculated that 0.34 Mt OC was stored in all Scottish sea lochs. In
24 comparison, our findings estimate that Loch Sunart alone holds 11.05 Mt OC. However,
25 Burrows et al. (2014) focused on the top 10 cm of sediment because data availability and the
26 lack of a robust methodology made it impossible to calculate the entire sedimentary C stock;
27 this has resulted in a significant underestimation of the quantity of C held within the sediment
28 of these lochs. Additionally, Burrows et al. (2014) did not consider IC to be a major
29 component in these sediments; instead the authors focused on Scottish sea lochs largely as OC
30 stores. In contrast, our results demonstrate that Loch Sunart stores 15.02 Mt IC in comparison
31 to 11.05 Mt OC. The general lack of IC data for Scottish sea lochs makes it difficult to assess
32 how representative Loch Sunart is of these coastal sedimentary IC stores; our results do



1 highlight the potential significance of IC as a major component of sedimentary C stores in
2 these depositional environments. Our results also highlight that sea lochs (and probably fjords
3 in general) act as an OC-rich sediment transition zone between terrestrial and oceanic
4 environments.

5 Loch Sunart's sediment currently holds 11.05 Mt OC which has been trapped and prevented
6 from reaching the adjacent shelf sea. This OC trapping in the coastal zone may reduce
7 reworking and remineralisation of the material which would have otherwise resulted in the
8 release of CO₂ through biotic processes (Smith et al., 2015). This 11.05 Mt OC is equivalent
9 to 40.93 Mt CO₂e (carbon dioxide equivalent). As a whole, the sediment within Loch Sunart
10 stores 99.56 Mt CO₂e which is almost double Scotland's total greenhouse gas emission for
11 2013 which reached an estimated 53 Mt CO₂e (Scottish Government, 2015).

12 Globally, the terrestrial C stores have received much more attention than their marine
13 counterparts; with significant focus on quantifying the forest (Köhl et al., 2015) and soil C
14 stocks (Köchy et al., 2015, Scharlemann et al., 2014). The work by Duarte et al. (2005) to
15 compile the known stocks and burial rate of C in the coastal environment highlighted that the
16 coastal ocean is a large store of carbon, which remains poorly understood; from this work the
17 concept of Blue Carbon arose (Nellemann et al., 2009). The focus of Duarte et al. (2005) was
18 to highlight that the vegetated coastal zones (i.e. saltmarsh, seagrass and mangroves) bury and
19 store significant quantities of C and that these stores should be further investigated and
20 recognised in policy outputs, but they largely overlooked the importance of what they
21 described as depositional area (estuaries and the shelf sea) as long-term repositories of OC
22 detritus from the vegetated coastal environment (Krumhansl et al. 2012). These authors
23 recognised that coastal (and shelf?) depositional areas are important stores of sedimentary C
24 globally, yet no consideration is given to how these areas vary in terms of their capacity to
25 store C. Conceptually, if we consider the types of estuaries (i.e. fjord, delta, coastal plain, bar-
26 built and tectonic), it is clear that the characteristics of each type of estuary will impact the
27 manner in which C is buried and stored, for example the restricted nature of fjords will be
28 conducive to sediment capture and C storage compared to the more open estuarine types.

29 Our initial work suggests that the depositional area category could be further expanded upon
30 to include fjords as a separate component and this concept is supported by Smith et al. (2015),
31 who indicated that fjords are "hot-spots for OC burial" and should be considered separately
32 from estuaries when investigating global ocean OC burial. Currently, there is insufficient data



1 globally to advocate fjords being categorised as a separate component in global coastal C
2 stores; the standardised methodology outlined (Fig.4) provides a platform to investigate this
3 concept further.

4 At the national level there has been a significant focus on quantifying Scottish soil C stocks,
5 with much attention given to the peatlands (Aitkenhead & Coull., 2016, Bradley et al., 2005
6 & Chapman et al. 2009). Peat and other organic rich soils cover 66% of Scotland and account
7 for 50% of all the United Kingdom's soil C stocks (Cummins et al., 2011). The Scottish
8 peatlands store 1620 Mt C (Chapman et al., 2009) over an area of 17270 km², while the other
9 soils hold 2110.9 Mt C over 60215 km² (Aitkenhead & Coull., 2016). In comparison to these
10 figures, the quantity of C stored in Loch Sunart is small, but the loch itself only covers an area
11 of 47.3 km². When the loch's C_{eff} is compared to how effectively Scotland's soils and
12 peatland store C (Table.5) we can see that on a C amount per unit area basis Loch Sunart
13 stores significantly more C than the soils of Scotland. The loch has a C_{eff} of 0.568 Mt C km⁻²
14 compared to 0.094 Mt C km⁻² and 0.035 Mt C km⁻² for the peatlands and other soils of
15 Scotland. Our results suggest that Loch Sunart is one of the most effective stores of C in
16 Scotland and highlights the potential of the sediment in these sea lochs to hold a significant
17 quantity of C which has previously not been recognised. Many of these terrestrial C stores
18 are, of course, vulnerable to rapid and long-term environmental change; the Scottish terrestrial
19 C stocks are at risk from erosion (Cummins et al. 2011) and even fire (Davies et al. 2013),
20 both of which are increasing in pace and frequency by anthropogenic activities. In
21 comparison, a sea loch's geomorphology combined with its depth gives sedimentary C stores
22 a level of protection not afforded to terrestrial C stores. This does not mean that the
23 sedimentary C in sea lochs is invulnerable, but rather that it is buffered from the immediate
24 effects of chemical, biological and physical environmental change. Little is currently known
25 regarding the long-term stability of these stores.

26 The methodology outlined in this paper has given us a platform to calculate the carbon stocks
27 within Loch Sunart and has the potential to be applied in other fjordic systems as well as
28 environments with restricted sediment exchange processes, such as estuaries and freshwater
29 lakes, as well as artificial systems such as reservoirs and irrigation pools.

30 **5 Conclusion**

31 The integration of the geochemical and geophysical techniques outlined provides a robust and
32 repeatable methodology to quantitatively calculate the volume of sediment and make first



1 order estimations of carbon stored within fjordic sediments. Using this methodology we have
2 shown that Loch Sunart holds 26.88 Mt C which is almost double the quantity of Scottish
3 CO₂ emissions for 2013. Although this is small in comparison with Scotland's peatland and
4 soil C stocks, per unit area Loch Sunart is a more effective store of both OC and IC than
5 Scotland's soils or peatlands. The results from this study suggest that the sediment in
6 Scotland's 110 sea lochs (Edwards and Sharples et al., 1986) represent a potentially
7 significant, yet currently largely unaccounted for repository for both OC and IC. These
8 coastal settings trap and prevent the remineralisation of OC into the atmosphere. Additionally,
9 the C held within these 110 sea lochs is likely to represent a significant part of Scotland's blue
10 carbon capital that has not been considered at the marine ecosystem, global C cycle and wider
11 policy levels. Without a better understanding of these stores of marine sedimentary C we will
12 remain unable to fully quantify the coastal C cycle or the role that these fjordic environments
13 play in buffering the release of CO₂ through the burial of C in these sediments. The future
14 strategic use of this methodology within different fjord types and locations offers the potential
15 to upscale and quantify the C held within all Scottish sea lochs and possibly begin to estimate
16 the fjordic sedimentary C stores both at a national and global level.

17 **Author Contribution**

18 CS & WA conceived the research and wrote the initial manuscript, to which all co-authors
19 contributed data or provided input. CS conducted the research as part of his PhD at the
20 University of St Andrews, supervised by WA, AD and JH.

21 **Acknowledgements**

22 This work was supported by the Natural Environment Research Council [Grant Number:
23 NE/L501852/1] with additional support from the NERC Radiocarbon Facility [Allocation
24 1934.1015]. Seismic profiles and the CALYPSO long core were acquired within the frame of
25 the French ECLIPSE program. The authors would like to thank Marion Dufresne's Captain J.-
26 M. Lefevre, the Chief Operator Y. Balut (from IPEV) and Richard Bates (University of St
27 Andrews). Additionally; we would like to thank Colin Abernethy (Scottish Association of
28 Marine Science) for laboratory support.



1 **References**

- 2 Aitkenhead, M. J. and Coull, M. C.: Mapping soil carbon stocks across Scotland using a
3 neural network model, *Geoderma*, 262, 187–198, doi:10.1016/j.geoderma.2015.08.034, 2016.
- 4 Baeten, N. J., Forwick, M., Vogt, C. and Vorren, T. O.: Late Weichselian and Holocene
5 sedimentary environments and glacial activity in Billefjorden, Svalbard, *Geol. Soc. London,*
6 *Spec. Publ.*, 344(1), 207–223, doi:10.1144/SP344.15, 2010.
- 7 Baltzer, A., Bates, C.R., Mokeddem, Z., Clet-Pellerin, M., Walter-Simonnet, A-V., Bonnot
8 Courtois, C. and Austin, W.E.N. Using seismic facies and pollen analyses to evaluate
9 climatically driven change in a Scottish sea loch (fjord) over the last 20 ka, *Geological*
10 *Society, London, Special Publications*, 344, (1), pp. 355–369, 2010
- 11 Bauer, J.E., Cai, W-J, Raymond, P.A., Bianchi, T.S., Hopkinson, C.S., and Regnier, P.A.G.
12 2013, The changing carbon cycle of the coastal ocean., *Nature*, 504, (7478), pp. 61–70, 2013
- 13 Bates, C.R., Moore, C.G., Harries, D.B., Austin, W.E.N., and Lyndon, A. R. Broad scale
14 mapping of sublittoral habitats in Loch Sunart, Scotland. Scottish Natural Heritage
15 Commissioned. Report No. 006 (ROAME No. F01AA401C), 2004.
- 16 Binns, P. E., Harland, R. & Hughes, M. J. 1974a. Glacial and post glacial sedimentation in the
17 sea of the Hebrides. *Nature*, 248, 751–754, 1974a.
- 18 Binns, P. E., Mcquillin, R. & Kenolty, N. 1974b. The geology of the sea of the Hebrides.
19 Institute of Geological Sciences 73/14, 1974b.
- 20 Boulton, G. S., Chroston, P.N. & Jarvis, J. A marine seismic study of late Quaternary
21 sedimentation and inferred glacier fluctuations along western Inverness–shire, Scotland.
22 *Boreas*, 10, 39–51, 1981.
- 23 Bond, C. E., Gibbs, A. D., Shipton, Z. K. and Jones, S.: What do you think this is?
24 “Conceptual uncertainty” In geoscience interpretation, *GSA Today*, 17(11), 4–10,
25 doi:10.1130/GSAT01711A.1, 2007.
- 26 Bradley, R.I., Milne, R., Bell, J., Lilly, A., Jordan, C. and Higgins, A.. A soil carbon and land
27 use database for the United Kingdom. *Soil Use and Management*, 21, 363–369, 2005
- 28 Bronk Ramsey, C. Bayesian analysis of radiocarbon dates. *Radiocarbon*, 51(1), 337–360,
29 2009



- 1 Bronk Ramsey, C. and Lee, S. Recent and planned developments of the program OxCal.
- 2 Radiocarbon, 55(2-3), 720-730, 2013
- 3 Burrows M.T., Kamenos N.A., Hughes D.J., Stahl H., Howe J.A. and Tett P. Assessment of
- 4 carbon budgets and potential blue carbon stores in Scotland's coastal and marine
- 5 environment. Scottish Natural Heritage Commissioned Report No. 761, 2014
- 6 Cage, A.G., Heinemeier, J. and Austin, W.E.N. Marine radiocarbon reservoir ages in Scottish
- 7 coastal and fjordic waters, Radiocarbon, Vol 48, Nr 1, 31–43, 2006.
- 8 Cai, W.-J.: Estuarine and coastal ocean carbon paradox: CO₂ sinks or sites of terrestrial
- 9 carbon incineration?, Ann. Rev. Mar. Sci., 3, 123–45, doi:10.1146/annurev-marine-120709-
- 10 142723, 2011.
- 11 Capell, R., Tetzlaff, D. and Soulsby, C.: Will catchment characteristics moderate the
- 12 projected effects of climate change on flow regimes in the Scottish Highlands?, ,
- 13 699(December 2012), 687–699, doi:10.1002/hyp.9626, 2013.
- 14 Cannell, M.G.R., Milne, R., Hargreaves, K.J., Brown, T.A.W., Cruickshank, M.M., Bradley,
- 15 R.I., Spencer, T., Hope, D., Billett, M.F., Adger, W.N. and Subak, S. National inventories of
- 16 terrestrial carbon sources and sinks: The UK experience. Climatic Change, 42, 505–530, 1999
- 17 Clark, C. D., Hughes, A. L. C., Greenwood, S. L., Jordan, C. and Petter, H.: Pattern and
- 18 timing of retreat of the last British-Irish Ice Sheet, Quat. Sci. Rev.,
- 19 doi:10.1016/j.quascirev.2010.07.019, 2010.
- 20 Chapman, S.J., Bell, J.S., Campbell, C.D., Hudson, G, Lilly, A., Nolan, A.J., Robertson,
- 21 A.H.J., Potts, J.M., and Towers, W, Comparison of soil carbon stocks in Scottish soils
- 22 between 1978 and 2009, European Journal of Soil Science, 64, (4), pp. 455–465, 2013
- 23 Chapman, S.J., Bell, J., Donnelly, D. and Lilly, A., Carbon stocks in Scottish peatlands, Soil
- 24 Use and Management, 25, (2), pp. 105–112, 2009.
- 25 Chiles, J.P., and Delfiner.P. Geostatistics: Modeling Spatial Uncertainty. John Wiley and
- 26 Sons, New York, 695, 1999.
- 27 Cressie, N.A.C. The Origins of Kriging, Mathematical Geology, v. 22, p. 239-252, 1990.
- 28 Cummins, R., Donnelly, D., Nolan, A., Towers, W., Chapman, S., Grieve, I. and Birnie, R.V.
- 29 Peat erosion and the management of peatland habitats. Scottish Natural Heritage
- 30 Commissioned Report No. 410, 2011



- 1 Dadey, K.A., Janecek, T. and Klaus, A Dry bulk density: its use and determination,
2 Proceedings of the Ocean Drilling Program, Scientific Results, Vol. 126, 1992.
- 3 Davies, G. M., Gray, A., Rein, G. and Legg, C. J.: Peat consumption and carbon loss due to
4 smouldering wildfire in a temperate peatland, *For. Ecol. Manage.*, 308, 169–177,
5 doi:10.1016/j.foreco.2013.07.051, 2013.
- 6 Duarte, C. M., Middelburg, J. J. and Caraco, N.: Major role of marine vegetation on the
7 oceanic carbon cycle, *Biogeosciences*, 2, 1–8, 2005.
- 8 Edwards, A. & Sharples, F. Scottish Sea Lochs: A Catalogue. Scottish Marine Biological
9 Association/ Nature Conservancy Council, Oban, 1986.
- 10 Forwick, M., Vorren, T. O., Hald, M., Korsun, S., Roh, Y., Vogt, C. and Yoo, K.-C.: Spatial
11 and temporal influence of glaciers and rivers on the sedimentary environment in
12 Sassenfjorden and Tempelfjorden, Spitsbergen, *Geol. Soc. London, Spec. Publ.*, 344(1), 163–
13 193, doi:10.1144/SP344.13, 2010.
- 14 Friedrich, J., Janssen, F., Aleynik, D., Bange, H. W., Boltacheva, N., Çagatay, M. N., Dale, a.
15 W., Etiopé, G., Erdem, Z., Geraga, M., Gilli, a., Gomoiu, M. T., Hall, P. O. J., Hansson, D.,
16 He, Y., Holtappels, M., Kirf, M. K., Kononets, M., Kononov, S., Lichtschlag, a.,
17 Livingstone, D. M., Marinaro, G., Mazlumyan, S., Naeher, S., North, R. P., Papatheodorou,
18 G., Pfannkuche, O., Prien, R., Rehder, G., Schubert, C. J., Soltwedel, T., Sommer, S., Stahl,
19 H., Stanev, E. V., Teaca, a., Tengberg, a., Waldmann, C., Wehrli, B. and Wenzhöfer, F.:
20 Investigating hypoxia in aquatic environments: Diverse approaches to addressing a complex
21 phenomenon, *Biogeosciences*, 11(4), 1215–1259, doi:10.5194/bg-11-1215-2014, 2014.
- 22 Gillibrand, P.A., Cage, A.G. and Austin, W.E.N. A preliminary investigation of basin water
23 response to climate forcing in a Scottish fjord: evaluating the influence of the NAO,
24 *Continental Shelf Research*, 25, (5-6), pp. 571–587, 2005
- 25 Hedges, J.I., Keil, R.G. and Benner, R. What happens to terrestrial organic matter in the
26 ocean? *Organic Geochemistry*, 27, 195–212, 1997.
- 27 Hilton, R.G., Galy, A., Hovius, N. & Horng, M.J. Efficient transport of fossil organic carbon
28 to the ocean by steep mountain rivers: An orogenic carbon sequestration mechanism. *Geology*
29 39, 71–74, 2011.



- 1 Hinojosa, J.L, Christopher M. Moy, C.M, Claudine H. Stirling, C.H, Gary S. Wilson, G.S,
2 and Eglinton, T.I : Carbon cycling and burial in New Zealand's fjords, , 4047–4063,
3 doi:10.1002/2014GC005433.Received, 2014.
- 4 Howard, P.J.A., Loveland, P.J., Bradley, R.I., Dry, F.T., Howard, D.M. and Howard, D.C..
5 The carbon content of soil and its geographical distribution in Great Britain. *Soil Use and*
6 *Management*, 11, 9–15, 1995.
- 7 Howe, J. A., Shimmiel, T., Austin, W. E. N. and Longva, O.: Post-glacial depositional
8 environments in a mid-high latitude glacially-overdeepened sea loch , inner Loch Etive ,
9 western Scotland, , 185, 417–433, 2002.
- 10 Johnston, D.H and R. Cooper, M.R., *Methods and Applications in Reservoir Geophysics*,
11 *Investigations in geophysics*, no. 15., Tulsa, OK : Society of Exploration Geophysicists, 2010.
- 12 Kennedy, P., Kennedy, H., and Papadimitriou, S. The effect of acidification on the
13 determination of organic carbon, total nitrogen and their stable isotopic composition in algae
14 and marine sediment, *Rapid Communications in Mass Spectrometry*, 19, (8), pp. 1063–1068,
15 2005.
- 16 Köchy, M., Hiederer, R. and Freibauer, A.: Global distribution of soil organic carbon – Part 1:
17 Masses and frequency distributions of SOC stocks for the tropics, permafrost regions,
18 wetlands, and the world, *Soil*, 1(1), 351–365, doi:10.5194/soil-1-351-2015, 2015.
- 19 Köhl, M., Lasco, R., Cifuentes, M., Jonsson, ??rjan, Korhonen, K. T., Mundhenk, P., de Jesus
20 Navar, J. and Stinson, G.: Changes in forest production, biomass and carbon: Results from the
21 2015 UN FAO Global Forest Resource Assessment, *For. Ecol. Manage.*, 352, 21–34,
22 doi:10.1016/j.foreco.2015.05.036, 2015
- 23 Krumhansl, K. A. and Scheibling, R. E.: Production and fate of kelp detritus, *Mar. Ecol. Prog.*
24 *Ser.*, 467, 281–302, doi:10.3354/meps09940, 2012
- 25 Mokeddem, Z., Baltzer, A., Goubert, E and Clet-Pellerin, M., A multiproxy
26 palaeoenvironmental reconstruction of Loch Sunart (NW Scotland) since the Last Glacial
27 Maximum, *Geological Society, London, Special Publications*, 344, (1), pp. 341–353, 2010.
- 28 Nellemann C., Corcoran E., Duarte C.M., Valdés L., DeYoung C., Fonseca L., Grimsditch G.
29 (Eds.), *Blue Carbon: A Rapid Response Assessment*, United Nations Environment
30 Programme, GRID-Arendal, (2009).



- 1 Nieuwenhuize, J., Maas, Y.E.M., and Middelburg, J.J. Rapid analysis of organic carbon and
2 nitrogen in particulate materials. *Mar. Chem.* 45:217-224, 1994
- 3 Nørgaard-Pedersen, N., Austin, W. E. N., Howe, J. a. and Shimmield, T.: The Holocene
4 record of Loch Etive, western Scotland: Influence of catchment and relative sea level changes,
5 *Mar. Geol.*, 228(1-4), 55–71, doi:10.1016/j.margeo.2006.01.001, 2006.
- 6 Pedersen, J. B. T., Kroon, a., Jakobsen, B. H., Mernild, S. H., Andersen, T. J. and Andresen,
7 C. S.: Fluctuations of sediment accumulation rates in front of an Arctic delta in Greenland,
8 *The Holocene*, 23(6), 860–868, doi:10.1177/0959683612474480, 2013.
- 9 Pergamon Press, 119–41 Polson, D. and Curtis, A.: Dynamics of uncertainty in geological
10 interpretation, *J. Geol. Soc. London.*, 167(1), 5–10, doi:10.1144/0016-76492009-055, 2010.
- 11 Press, W.H., Flannery, B.P., Teukolsky, S.A., and Vetterling, W.T. *Numerical Recipes in C*,
12 Cambridge University Press, 1988.
- 13 Reimer, P, *IntCal13 and Marine13 Radiocarbon Age Calibration Curves 0–50,000 Years cal*
14 *BP, Radiocarbon*, 55, (4), pp. 1869–1887, 2013.
- 15 Scottish Government. 2015. <http://www.gov.scot/Publications/2015/06/1939>; Accessed
16 25/11/2015.
- 17 Scharlemann, J. P., Tanner, E. V., Hiederer, R. and Kapos, V.: Global soil carbon:
18 understanding and managing the largest terrestrial carbon pool, *Carbon Manag.*, 5(1), 81–91,
19 doi:10.4155/cmt.13.77, 2014.
- 20 Scourse, J. D., Haapaniemi, A. I., Colmenero-hidalgo, E., Peck, V. L., Hall, I. R., Austin, W.
21 E. N., Knutz, P. C. and Zahn, R.: Growth, dynamics and deglaciation of the last British –
22 Irish ice sheet: the deep-sea ice-rafted detritus record, *Quat. Sci. Rev.*, 28(27-28), 3066–3084,
23 doi:10.1016/j.quascirev.2009.08.009, 2009
- 24 Soil Survey of Scotland Staff. (1970-1987). *Soil maps of Scotland (partial coverage) at a scale*
25 *of 1:25 000*. Macaulay Institute for Soil Research, Aberdeen.
- 26 Simpkin, P.G. and Davis, A. For seismic profiling in very shallow water, a novel receiver. In
27 *Sea Technology*, 1983.
- 28 Smith, R.W., Bianchi, T.S., Allison, M., Savage, C. & Galy, V, High rates of organic carbon
29 burial in fjord sediments globally, *Nature*, doi: 10.1038/NGEO2421, 2015.



- 1 Syvitski, J.P.M, Burrell, D.C & Skei, J.M. Fjords, Processes and Products, Springer-Verlag
- 2 New York, 1987.
- 3 Syvitski, J.P.M & Shaw, J: Sedimentology and Geomorphology of Fjords, Geomorphology
- 4 and Sedimentology of Estuaries. Developments in Sedimentology 53, 1995.
- 5 Wilson, L. J., Austin, W. E. N. and Jansen, E.: The last British Ice Sheet : growth , maximum
- 6 extent and deglaciation, , (2001), 243–250, 2002.
- 7 Verardo, D.J., P. N. Froelich, P.N. and McIntyre, A, Determination of organic carbon and
- 8 nitrogen in marine sediments using the Carlo Erba NA-1500 Analyzer. Deep Sea Res. 37:157-
- 9 165, 1990
- 10 Yu, Z, Loisel, J., Brosseau, D.P., Beilman, D.W., & Hunt, S.J. Global peatland dynamics
- 11 since the Last Glacial Maximum. Geophysical Research Letters 37, L13402, 2010.
- 12
- 13
- 14
- 15
- 16
- 17
- 18
- 19
- 20
- 21
- 22
- 23
- 24
- 25
- 26
- 27
- 28



1 **Table.1.** Details of the sediment cores extracted from Loch Sunart that were used in this study.

Core ID	Basin	Position (Lat, Long)	Water Depth (m)	Recovery (m)
GC009	Middle	56.672056, -5.867083	107	1.41
GC011	Outer	56.759861, -5.969639	91	2.45
GC013	Inner	56.681306, -5.629528	58	1.67
GC016	Inner	56.680944, -5.642333	58	0.56
GC020	Middle	56.704278, -5.751333	105	2.38
GC022	Middle	56.680333, -5.804944	120	2.46
GC023	Middle	56.665917, -5.840361	87	2.89
GC081	Middle	56.668972, -5.863278	58	3.63
GC01	Middle	56.696806, -5.704972	42	0.21
MD04 2833	Middle	56.665500, -5.859667	38	12

2

3

4

5

6

7

8

9

10

11

12

13

14

15

16

17

18

19

20



1 **Table.2** Radiocarbon ages from Loch Sunart cores. Ages were calibrated using OxCal 4.2.4 (Bronk
 2 Ramsey., 2009 & Bronk Ramsey & Lee., 2013) with the Marine13 curve (Reimer et al. 2013) and
 3 regional correction of ΔR value of -26 ± 14 yr (Cage et al. 2006) . All ages are calibrated at 95.4%
 4 probability and the mean age has been determined from the minimum and maximum calibrated ages.
 5 Additionally; we list the seismic unit assigned to each equivalent (eqv.) depth of each sample and
 6 compare this to the age equivalent seismic unit based on Baltzer et al. (2010).

Laboratory Code	Core ID	Depth (cm)	^{14}C Age, BP (No Correction)	Calibrated ^{14}C Age (cal BP)	Seismic Unit	Depth eqv.	Age eqv.
AA-48108	GC009	140	9827 \pm 49	10801 \pm 93		U2	U2
SUERC 65990	GC011	60	2837 \pm 35	2625 \pm 66		U3	U3
SUERC 65991	GC011	120	9890 \pm 38	10878 \pm 87		U2	U3
SUERC 65992	GC011	170	11266 \pm 40	12760 \pm 61		U2	U2
AA-48109	GC011	231	12181 \pm 58	13658 \pm 90		U1	U1
AA-48107	GC013	113	1716 \pm 32	1294 \pm 35		U3	U3
SUERC 65995	GC016	30	1865 \pm 35	1438 \pm 51		U3	U3
SUERC 65994	GC020	9	683 \pm 35	357 \pm 44		U3	U3
SUERC 65993	GC020	19	3067 \pm 37	2864 \pm 57		U3	U3
AA-48106	GC020	126	11652 \pm 74	13160 \pm 90		U2	U2/U1
AA-51569	GC023	30	340 \pm 60	64 \pm 51		U3	U3
SUERC-681	GC023	49	1215 \pm 47	788 \pm 58		U3	U3
SUERC-677	GC023	58	1322 \pm 43	886 \pm 55		U3	U3
AA-51570	GC023	73	1430 \pm 55	1011 \pm 66		U3	U3
SUERC-679	GC023	111.5	1695 \pm 57	1274 \pm 59		U2	U3
SUERC-680	GC023	250	2180 \pm 61	1801 \pm 80		U2	U3
CAMS-82821	GC023	286	2425 \pm 40	2099 \pm 70		U2	U3
UL 2853	MD04-2833	745	14420 \pm 210	17041 \pm 312		U1	U1

7

8

9

10

11

12

13

14

15

16

17



1 **Table.3** Sediment volume calculated as the mean of the three numerical integration algorithms; the
 2 error is reported as relative standard deviation (%RSD) which integrates the uncertainty in the seismic
 3 interpolation and the standard deviation of the numerical integration algorithms. The data is reported
 4 for the post-glacial (PG) and glacial (G) sediment at the basin level.

Basin	Layer	Volume	
		Mean (m ³)	%RSD
Inner	PG	2869825.90	6.48
	G	1301836.56	1.89
Middle	PG	23046267	7.26
	G	7363034.04	1.89
Outer	PG	13371884	7.90
	G	2667373.2	1.89
Loch Sunart	PG	530872293	7.39
	G	599731882	1.89
	Total	1130604175.55	3.61

5

6

7

8

9

10

11

12

13

14

15

16

17

18

19

20

21

22



1 **Table.4** Mass of sediment held within Loch Sunart and the mass of total carbon (TC), organic carbon
2 (OC) and inorganic carbon (IC) held with Loch Sunart's Sediment.

Basin	Layer	Mass (Mt)	TC (Mt)	OC (Mt)	3
					IC (Mt)
Inner	PG	27.05 ± 2.98	1.31 ± 0.16	1.05 ± 0.14	0.26 ± 0.15
	G	126.65 ± 7.15	0.81 ± 0.62	0.24 ± 0.2	0.57 ± 0.45
Middle	PG	421.53 ± 7.26	14.08 ± 0.30	7.05 ± 0.25	7.03 ± 0.17
	G	738.31 ± 9.62	3.97 ± 0.88	1.17 ± 0.28	2.80 ± 0.56
Outer	PG	203.52 ± 11.10	4.49 ± 0.34	1.32 ± 0.14	3.15 ± 0.24
	G	411.22 ± 9.78	2.21 ± 0.84	0.65 ± 0.14	1.56 ± 0.57
Loch Sunart	PG	652.09 ± 6.62	19.88 ± 0.27	8.98 ± 0.21	10.09 ± 0.17
	G	1276.17 ± 8.93	7.00 ± 0.82	2.07 ± 0.27	4.93 ± 0.58
Total		1928.26 ± 7.29	26.88 ± 0.52	11.05 ± 0.23	15.02 ± 0.35

10

11

12

13

14

15

16

17

18

19

20

21

22

23

24

25

26

27

28



1 **Table.5** The effective C storage (C_{eff}) of Loch Sunart's postglacial and glacial sediment in comparison
 2 to Scottish terrestrial C stores.

C Inventories	Area (km ²)	TC (Mt)	C_{eff} (Mt km ⁻²)	OC_{eff} (Mt km ⁻²)	IC_{eff} (Mt km ⁻²)	Reference
Postglacial						4
Inner Basin	5.5	1.31	0.238	0.191	0.047	5
Middle Basin	24.7	14.08	0.57	0.285	0.284	6
Outer Basin	17.1	4.49	0.263	0.077	0.184	7
Glacial						8
Inner Basin	5.5	0.81	0.147	0.044	0.104	9
Middle Basin	24.7	3.97	0.161	0.047	0.113	10
Outer Basin	17.1	2.21	0.129	0.038	0.091	11
Postglacial	47.3	19.88	0.42	0.189	0.213	12
Glacial	47.3	7.00	0.148	0.044	0.104	13
Loch Sunart	47.3	26.88	0.568	0.234	0.318	14
2 m Depth						15
Peatlands*	17270	1620		0.094		Chapman et al., 2009
Organo-Mineral Soil*		754				Bradley et al., 2005
Mineral Soil*		498				16
1 m Depth						17
Peat	17369	813.9		0.047		Aitkenhead & Coull, 2016
Alluvial Soil	1657	40.8		0.025		18
Alpine Soil	3825	145.7		0.038		19
Bare Ground	1672	50.5		0.030		20
Brown Earth	15971	590.3		0.037		21
Gley	15963	645.4		0.040		22
Podzol	18159	536.6		0.029		23
Ranker	2531	82.6		0.033		24
Regosol	437	19.0		0.044		25

20 *Both studies calculated the soil C stocks excluding IC data therefore the stocks only represent the OC
 21 held within these stocks.

22

23

24

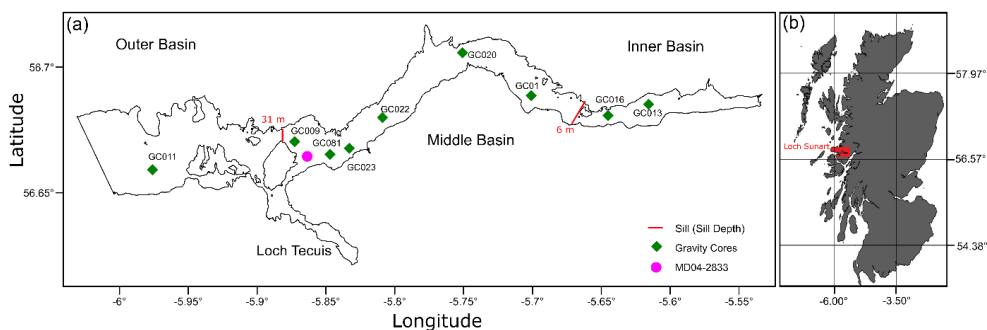
25

26

27

28

29



1

2 **Figure 1.** Maps of Loch Sunart illustrating (a) the three basins and the sediment core

3 locations (b) Loch Sunart in a Scottish context.

4

5

6

7

8

9

10

11

12

13

14

15

16

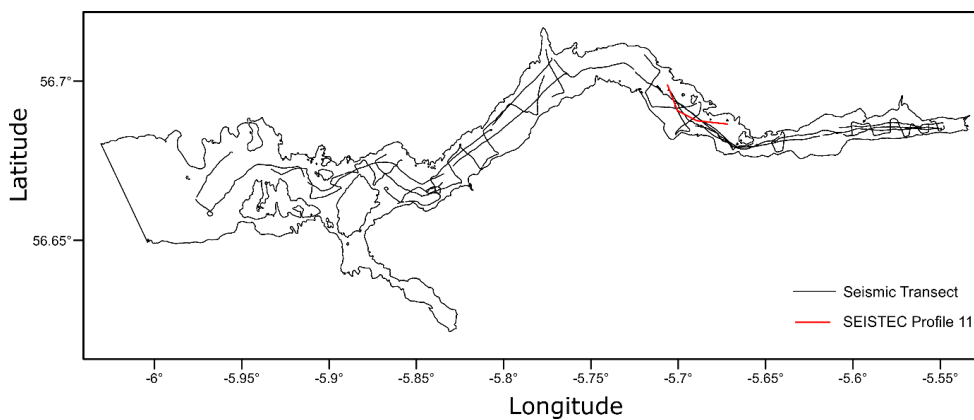
17

18

19

20

21



1

2 **Figure.2.** Map of the 34 Seismic transects undertaken in Loch Sunart with Siestec Profile 11
3 highlighted.

4

5

6

7

8

9

10

11

12

13

14

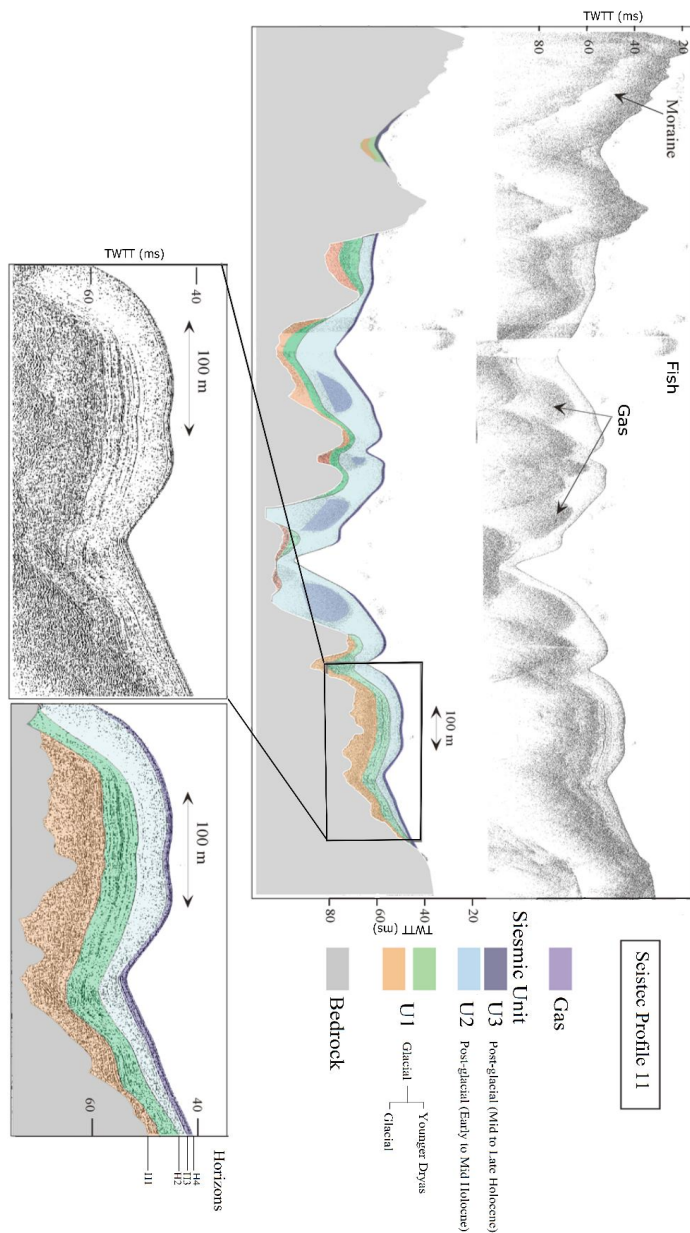
15

16

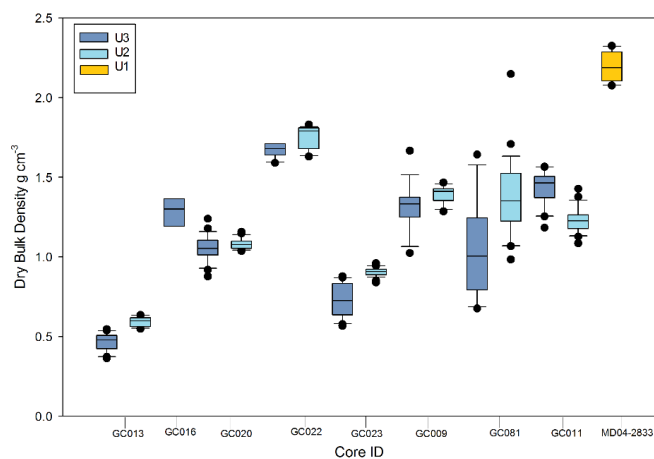
17

18

19



1
 2 **Figure 3.** SIESTEC Profile 11: A characteristic seismic profile displaying the four seismic
 3 horizons (H1, H2, H3 and H4) and the three seismic units (U1, U2 and U3) adapted from
 4 Baltzer et al.,2010.



1

2 **Figure 4.** Dry bulk density values from each sediment cores corresponding to seismic units 1,
3 2 and 3.

4

5

6

7

8

9

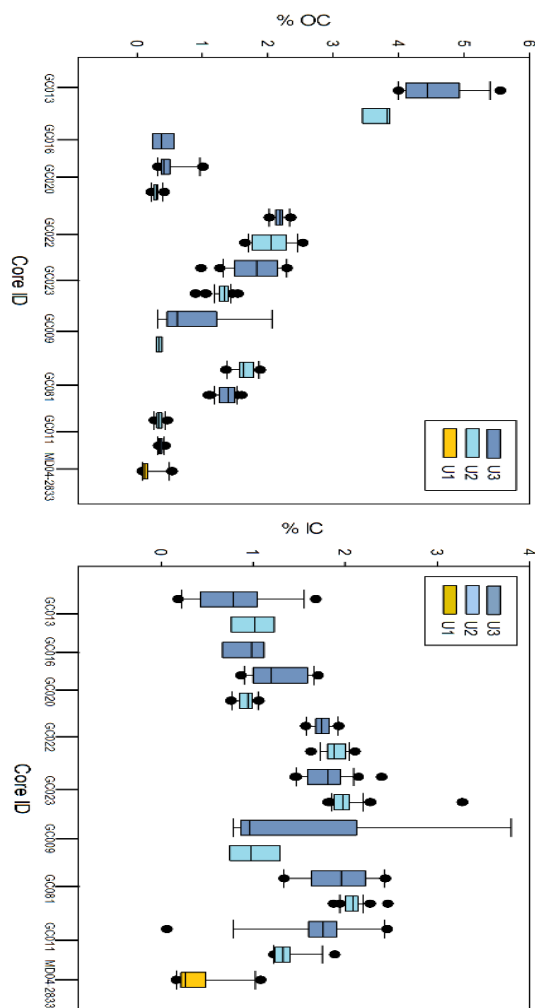
10

11

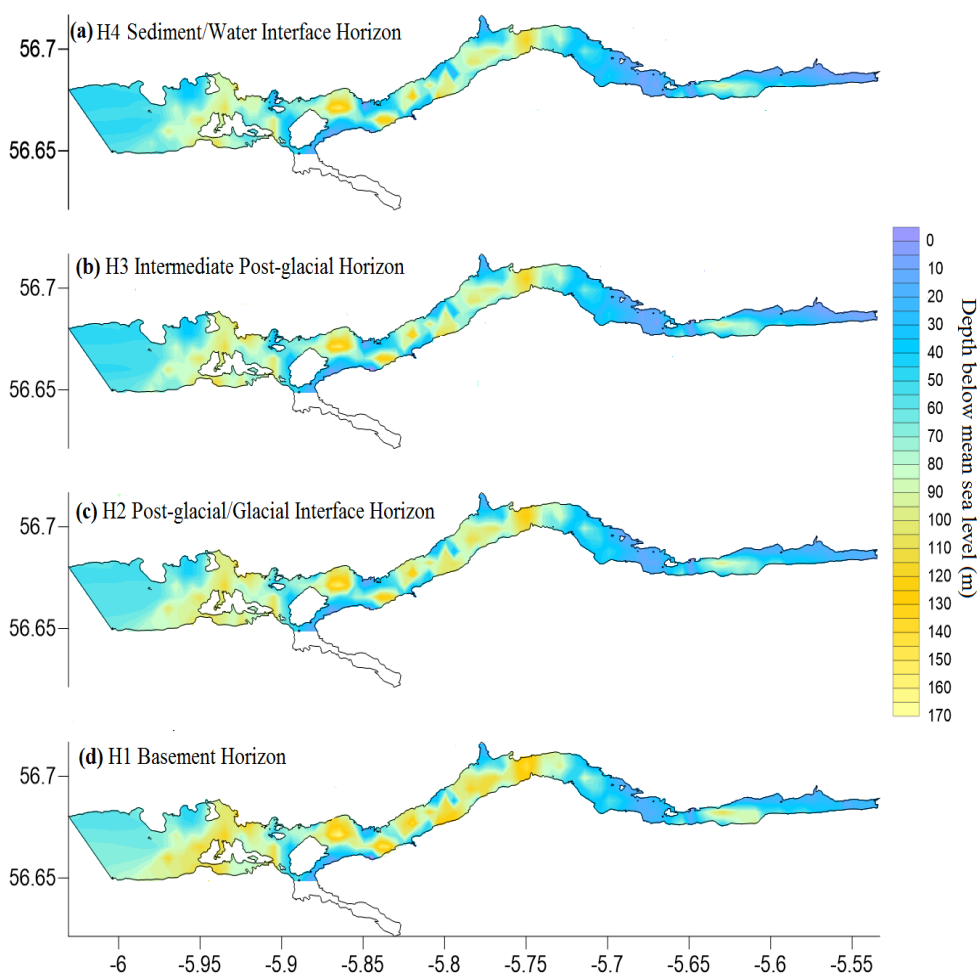
12

13

14



1
 2 **Figure 5.** %OC and %IC values from each sediment cores corresponding to seismic units 1, 2
 3 and 3.



1

2 **Figure 6.** Contour maps defining the topography of each seismic horizon. **(a)** H4
3 sediment/water interface. **(b)** H3 intermediate post-glacial horizon. **(c)** H2 post-glacial/glacial
4 interface. **(d)** H1 basement.

5

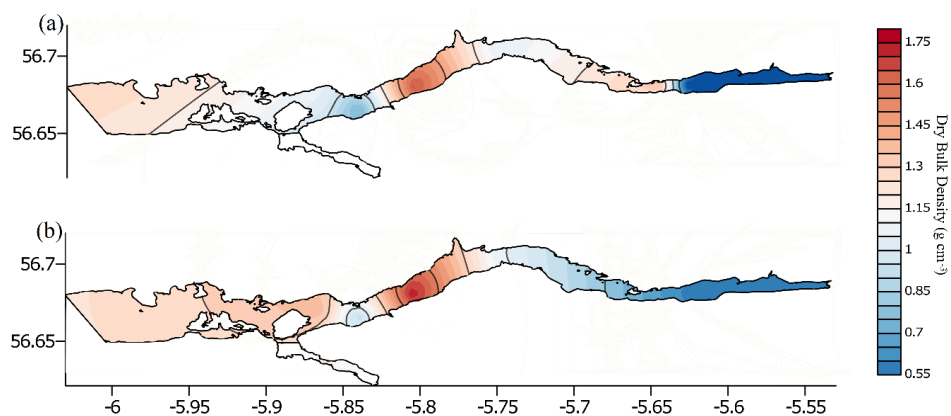
6

7

8

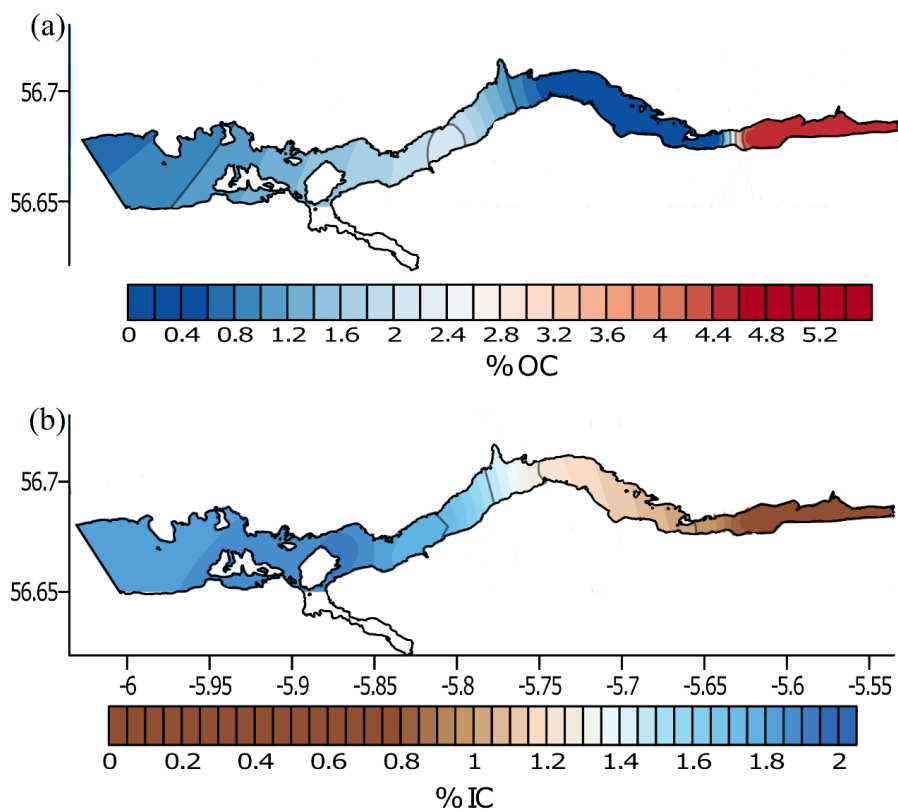
9

10



1
2 **Figure 7.** Contour maps showing the output of the spatial distribution model for the mean
3 dry bulk density of (a) U3. (b) U2.

4
5
6
7
8
9
10
11
12
13
14
15
16
17
18
19



1

2 **Figure 8.** Output of U3 spatial distribution model for (a) Total carbon. (b) Organic carbon.
3 (c) Inorganic carbon.

4

5

6

7

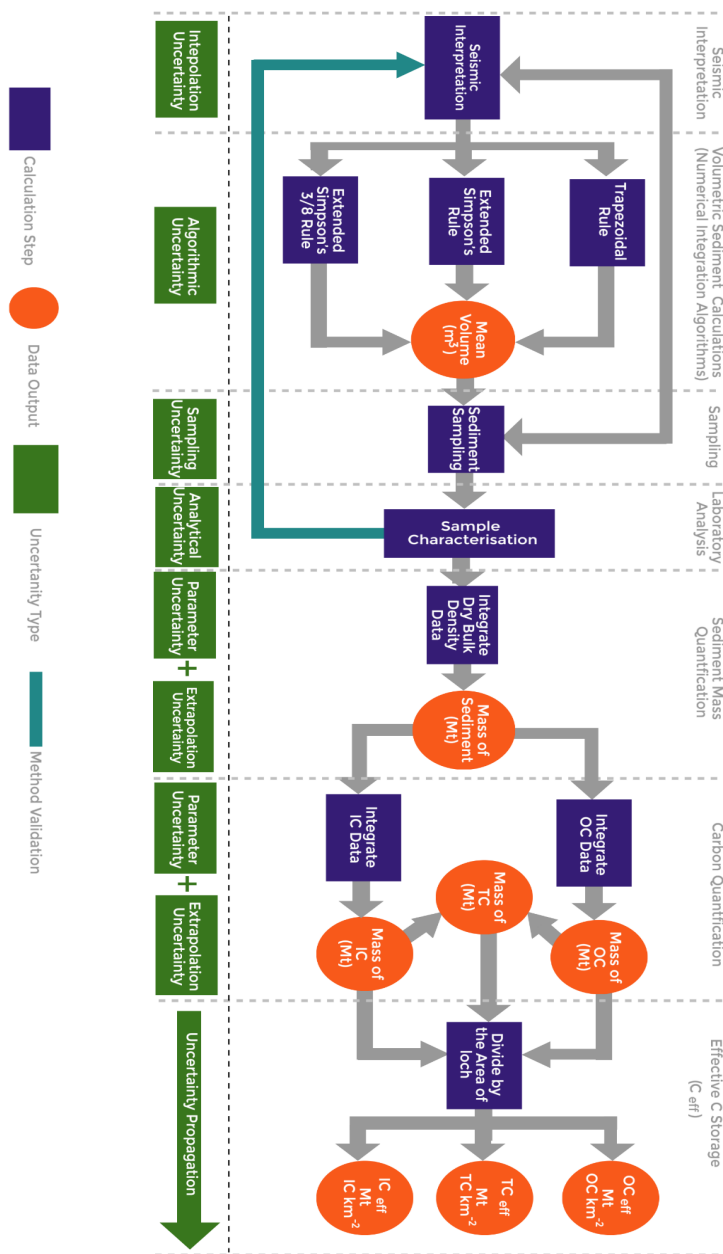
8

9

10

11

12



1

2 **Figure 9.** Flow diagram detailing the steps towards calculating the sedimentary C stocks
 3 within a fjord with the known uncertainties specified.